Wind and Structures, Vol. 9, No. 2 (2006) 147-158
DOI: http://dx.doi.org/10.12989/was.2006.9.2.147

Computational fluid dynamics simulation of pedestrian wind in urban area with the effects of tree

Cheng-Hsin Chang†

Department of Civil Engineering and Wind Engineering Research Center
Tamkang University, Tamsui, Taipei County, Taiwan

(Received August 17, 2005, Accepted March 7, 2006)

Abstract. The purpose of this paper is to find a more accurate method to evaluate pedestrian wind by computational fluid dynamics approach. Previous computational fluid dynamics studies of wind environmental problems were mostly performed by simplified models, which only use simple geometric shapes, such as cubes and cylinders, to represent buildings and structures. However, to have more accurate and complete evaluation results, various shapes of blocking objects, such as trees, should also be taken into consideration. The aerodynamic effects of these various shapes of objects can decrease wind velocity and increase turbulence intensity. Previous studies simply omitted the errors generated from these various shapes of blocking objects. Adding real geometrical trees to the numerical models makes the calculating domain of CFD very complicated due to geometry generation and grid meshing problems. In this case the function of Porous Media Condition can solve the problem by adding trees into numerical models without increasing the mesh grids. The comparison results between numerical and wind tunnel model are close if the parameters of porous media condition are well adjusted.

Keywords: CFD; porous media condition; pedestrian wind; wind tunnel.

1. Introduction

More and more studies take serious account of wind conditions in the modern cities, such as pedestrian comfort, pollutant dispersion, snow and dust accumulation, and etc. Wind conditions vary depend on meteorological data, upstream terrains, surrounding objects and adjacent buildings. Previous wind-tunnel experiments have been carried out with simplified models and more complex building combinations for investigation of pedestrian level comfort. Murakami, *et al.* (1979) performed wind-tunnel experiments for tall buildings surrounded by uniformly distributed square blocks. The results indicated influences on wind flows with respect to building height, street width, surrounding height, wind direction and other parameters. Jamieson, *et al.* (1992) reported the effect of architectural detailing on pedestrian-level wind speeds. The Stathopoulos and Wu's study (1995) gave the results of wind speeds affected by a number of parameters such as the spatial density of street blocks, the building height over surroundings, the relative location of buildings and the direction of approaching wind for the estimation of pedestrian-level wind environmental conditions

† Assistant Professor, E-mail: cc527330@mail.tku.edu.tw

in built-up regions. Chang (2001a) and Meroney (2001b) focused attention on the flow fields, building pressures and line source dispersion characteristics found for idealized three-dimensional urban arrays.

Advanced technology makes faster and more powerful computers, which allow computational fluid dynamics (CFD) procedures to apply to many experimental flow problems. Today, CFD applications to wind engineering problems place more concern on wind load of buildings, pollutant dispersion phenomena, and pedestrian winds. Several previous studies have compared measurements made from physical modeling with numerical predictions. Stathopoulos, *et al.* (1996) used the modified Navier-Stokes equations and $k-s$ turbulence models, SIMPLE algorithm, to simulate the Montreal location near the downtown campus of Concordia University for the assessment of pedestrian comfort. Stathopoulos and Wu (2004) claimed that computed results generally agree with the experimental data for most locations. Compared to the traditional wind tunnel testing, CFD has the potential to be more efficient, and its graphic presentation of wind flow fields is particularly attractive to architects and planners. With the advances in computing power and methods, CFD is expected to play more important role in predicting pedestrian wind conditions. He and Song (1999) simulated the pedestrian wind fields around urban area using large eddy simulation CFD model based on the weakly compressible flow equations. CFD provides the detailed wind flow data at every grid points and every time step at different wind conditions. This advantage gives more accurate evaluation to the wind effects on pedestrian winds compare with wind tunnel tests. Svensson and Haggkvist (1990) explored a two-equation turbulence, based on the $\kappa-\varepsilon$ model for canopy flow. Hiraoka (1993) introduced a turbulence model of a canopy flow which including drag body. Uchida and Ohya (1993) calculated atmospheric flow over complex terrain, mountain height under 1000 m, by numerical approaches. Murakami, *et al.* (1999) summarized the recent achievements in computational wind engineering and its application to wind climate in scales ranging from human to urban scale and indicated that CFD made it possible to carry out a comprehensive analysis which incorporated various physical processes as associated with wind climate in various scales. Ferreira, *et al.* (1999) reported the predicting results on pedestrian level comfort concerning the interference effect created by two auxiliary buildings located upstream of recreation area comprising seven pavilions. The comparison between the numerical and experimental sets of velocity results revealed good agreement. Recently, Mochida, *et al.* (2002) considered the effects of roadside trees within the street canyon by using CFD analyses. The similar effects of planted trees arrangement and the elevation of tree crowns were added to CFD models. Due to the windbreak effects of trees, the large recirculation and high wind speed regions were reduced.

This study uses Computational Fluid Dynamic (CFD) methods to examine wind flow around buildings and predicting pedestrian wind conditions. Many previous studies showed that the accuracy of CFD was very high but not perfect. Attempts have been made by various researchers to advance the CFD technique in wind engineering, with the hope that it will eventually replace the wind tunnel testing. However, many difficulties in turbulence simulation and other areas have limited CFD's applications. Previous numerical studies used only simplified geometric models to examine wind environmental problems. The blocking objects such as windbreak and trees had been simply ignored. The reason of doing this simplification was to reduce the calculating grid and save the simulation cost. The aerodynamic effects of these objects can decrease wind velocity and increase turbulence intensity. In this study, the effects of trees in urban area are being examined to have more accurate results in CFD simulation. This study used Porous Media Condition to present

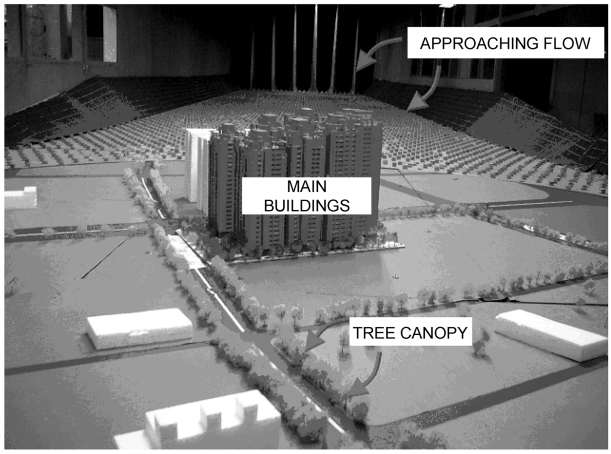

Fig. 1 Photographs of the completed model in wind tunnel

tree effects in the numerical model without increasing the mesh grid. The results of numerical and wind tunnel models were compared to evaluate the accuracy.

2. Case study and wind tunnel simulation

A wind-tunnel test of Sansifiga Building of the Great City Contracture CO., located at Sansia town, near Taipei County, Taiwan, was conducted to determine the pedestrian wind comfort. There were total 8 buildings with U shape arrangement. The average building height is around 95 m. The blue wooden models of eight building complex were fabricated to a 1:300 scale and centered on a turntable in the wind tunnel. Fig. 1 shows the photograph of the completed model in wind tunnel. The white styrofoam objects were constructed to represent surrounding buildings. The roadside trees were also considered in this study and were represented by the brown stuffs located at side roads and around blue wooden models in the picture.

The wind-tunnel test was performed in the environment boundary-layer wind tunnel of Tamkang University, Taipei Taiwan. This wind tunnel has an 18-m-long test section covered with roughness elements to reproduce at model scale the atmospheric wind characteristics required for the model test. The wind tunnel has a flexible roof, adjustable in height, to maintain a zero pressure gradient along the test section and to minimize blockage effects. An approach boundary layer representative of an suburban environment was established in the test section of the wind tunnel. The boundary layer had a mean wind speed profile power-law exponent of 0.18 and the mean velocity and turbulence intensity at model apex height were 15 m/s and 15%, respectively. Test Reynolds Number was approximately 3.06×10^5. These boundary layer characteristics were also the target values for inlet conditions to the test domain for the numerical calculations.

Measurements of pedestrian wind velocity were made for each Irwin Sensor location for 36 wind directions. The locations of the Irwin Sensor were chose by flow visualization observation. There were total 59 Irwin Sensors mounted on the turn table. Sensor 1 to 34 was located in the construction site. Fig. 2 shows the detailed locations of these sensors. The pedestrian wind velocities of the surrounding area were measured by sensor 35 to 59. Fig. 3 show the distribution of outer sensors.

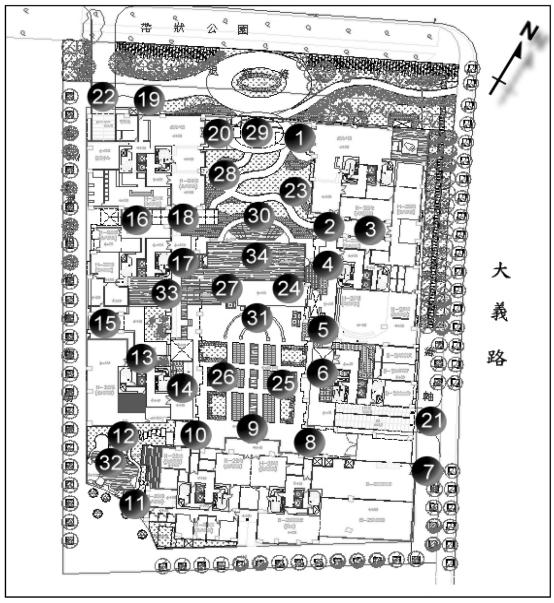

Fig. 2 Locations of Irwin sensor (inner site)

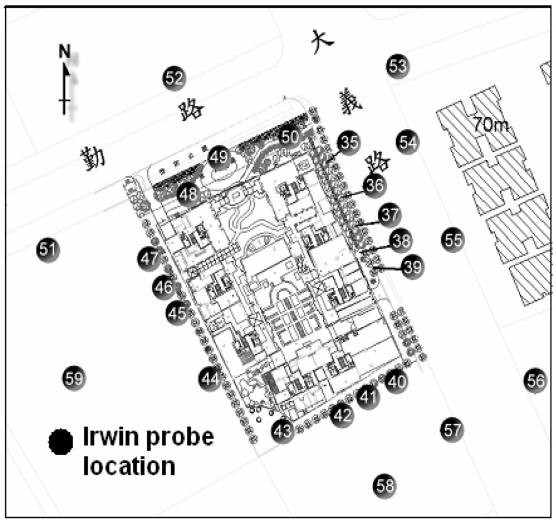

Fig. 3 Locations of Irwin sensor (outer site)

3. Numerical procedure

The numerical simulation tool used in this study was computational fluid dynamics, commercial code, Fluent. The Fluent CFD software was based on a finite volume discretization of the equations of motion, an unstructured grid volume made of either rectangular prisms or tetrahedral cells, various matrix inverting routines, and, in this case, either kappa-epsilon ($\kappa-\varepsilon$) or renormalized group theory kappa-epsilon (RNG-$\kappa-\varepsilon$) turbulence models. Steady state solutions were sought for

two configurations with and without the effects of roadside trees in calculation domains. The code was run on a dual Pentium Xeon 2.8 GHz PC using a Microsoft XP operating system with 2 GB Memory Ram.

3.1. Inlet conditions to the numerical domain

The velocity and turbulence intensity of the wind tunnel inlet flow can be used for calculating CFD inlet flow boundary conditions. The wind tunnel data and input profiles of velocity, turbulent kinetic energy, and dissipation used for the numerical simulation were chose same values. The inlet values of kinetic energy, k, and dissipation ratio, ε, are calculated from measured velocity profiles and turbulence intensities with a given friction velocity ratio, u_*/u_{ref} for the wind tunnel setup, according to Eq. (1) and Eq. (2).

Where, y is distance from the wall, κ is the von Karman constant.

$$k = \frac{3}{2}\sqrt{\overline{u'^2}} \tag{1}$$

$$\varepsilon = \frac{u_*^3}{\kappa y} \tag{2}$$

All velocity profiles are collinear, and the numerical and wind tunnel kinetic energy and dissipation ratio are very similar as well.

3.2. Numerical domain and roadside tree models

Version 6.0 of the FLUENT code was used for all numerical simulations. Inlet profiles were prepared by spreadsheet and save as inlet boundary condition file. The inlet mean velocity, turbulent kinetic energy and dissipation profiles were similar to those measured in the wind tunnel and in dynamic equilibrium with one another. The ground surface roughness measured during the laboratory experiments was 1.4×10^{-4} m or an equivalent sand roughness, k, equal to 4 mm. Values deduced from the numerical wind tunnel for these parameters were 1.7×10^{-4} m and 5 mm, respectively. All velocity profiles were essentially collinear, and the numerical and wind tunnel turbulence intensity values are also very similar. Two calculation domains were chosen, depending on with or without the effects of roadside trees in calculation domains. The functions of "Porous Media Condition" were added to represent trees in the case with tree consideration.

The typical numerical domain represented a 2 m wide wind tunnel, 1 m flow depth, and a 2 m test section length. The numerical domain contained some 235,411 cells, 489,832 faces and 50,005 nodes distributed over 12 face zones. Outlet and velocity inlet or symmetry boundaries were specified at the sides and top of the grid volume, while appropriate surface roughness was specified at the ground. The inflow boundary conditions were chosen to match the velocity and turbulence profiles measured during the wind-tunnel experiments. Outflow boundary conditions were chosen to maintain constant longitudinal rate of change of all dependent variables.

3.3. Porous media conditions

The porous media model can be used for a wide variety of problems including flows through

packed beds, filter papers, perforated plates, flow distributors, and tube banks. Trees were defined as a cell zone in which the porous media model was applied and the pressure loss in the flow was determined by input parameters. The porous media model incorporates with an empirically determined flow resistance in a region of model defined as "porous". In essence, the porous media model is nothing more than an added momentum sink in the governing momentum equations.

3.3.1. Momentum equations for porous media

Porous media are modeled by the addition of a momentum source term to the standard fluid flow equations. The source term is composed of two parts: a viscous loss term (Darcy, the first term on the right-hand side of Eq. (3), and an inertial loss term (the second term on the right-hand side of Eq. (4)

$$S_i = -\left(\sum_{j=1}^{3} D_{ij}\mu v_j + \sum_{j=1}^{3} C_{ij}\frac{1}{2}\rho v_{mag} v_j\right) \tag{3}$$

where S_i is the source term for the i^{th} (x, y, or z) momentum equation, and D and C were prescribed matrices. This momentum sink contributes to the pressure gradient in the porous cell, creating a pressure drop that is proportional to the fluid velocity (or velocity squared) in the cell.

To recover the case of simple homogeneous porous media

$$S_i = -\left(\frac{\mu}{\alpha} v_i + C_2\frac{1}{2}\rho v_{mag} v_i\right) \tag{4}$$

where α is the permeability, C_2 is the inertial resistance factor, and simply specify D and C as diagonal matrices with $1/\alpha$ and C_2, respectively, on the diagonals (and zero for the other elements). At high flow velocities, the constant C_2 in Eq. (2) provides a correction for inertial losses in the porous medium. This constant can be viewed as a loss coefficient per unit length along the flow direction, thereby allowing the pressure drop to be specified as a function of dynamic head.

3.3.2. Tree model and parameter setup

The aerodynamic effects of the roadside trees can decrease wind velocity and increase turbulence intensity. The geometrical shapes of branches and leaves are very complicated. Due to the grid meshing problem, it is very difficult to add trees to the numerical models. Porous media condition of FLUENT was used to simulate tree effects to solve this problem. For simple homogenous porous media condition, two parameters are needed, viscous resistance, C_2 and inertial resistance, $1/\alpha$, to find the momentum source term in Eq. (2). In turbulent flows, trees are modeled using both the permeability and an inertial loss coefficient. The permeability and inertial loss coefficient in each component direction may be identified as

$$\alpha = \frac{D_p^2}{150}\frac{\varepsilon^3}{(1-\varepsilon)^2}\ ;\ C_2 = \frac{3.5}{D_p}\frac{(1-\varepsilon)}{\varepsilon^3}$$

where, D_p : mean particle diameter

ε : void percentage

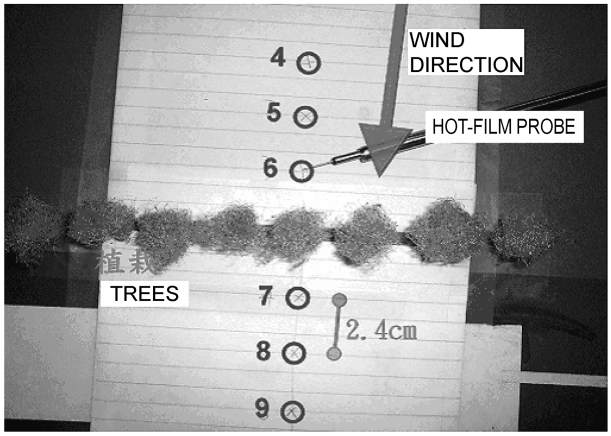

Fig. 4 Wind tunnel setup of velocity measurement by hot film probe

To determinate the values of C_2 and $1/\alpha$ for tree model for pedestrian wind simulation, a series of numerical simulations and wind tunnel test were performed. A simple wind tunnel test was held to obtain the variations of flow velocity before and after the flow passing the line arrangement of tree canopy. Fig. 4 is the picture of wind tunnel test. The hot-film probe measured the flow velocity for 12 locations at height of 1.6 cm along the line that perpendicular to the tree canopy. Similar CFD simulations were also performed by different parameter settings of Porous media for evaluating the best values of viscous resistance and inertial resistance. Fig. 5 shows the numerical simulation domain and the setup of the tree canopy models. Table 1 was the list of parameter of Porous media tested. The comparisons of CFD models and wind tunnel data were shown in Fig. 6

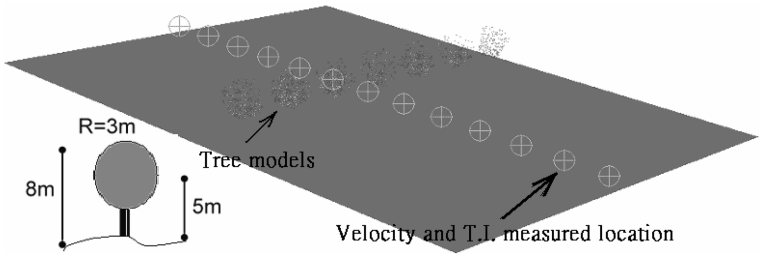

Fig. 5 Numerical simulation setup of the tree canopy model

Table 1 Porous parameter trial groups

Porous ID	D_p	ε	$1/\alpha$	C_2
1	0.1	0.8	1171.875	13.672
7	0.3	0.8	130.208	4.557
14	1	0.875	3.499	0.653
16	0.05	0.9	823.045	9.602

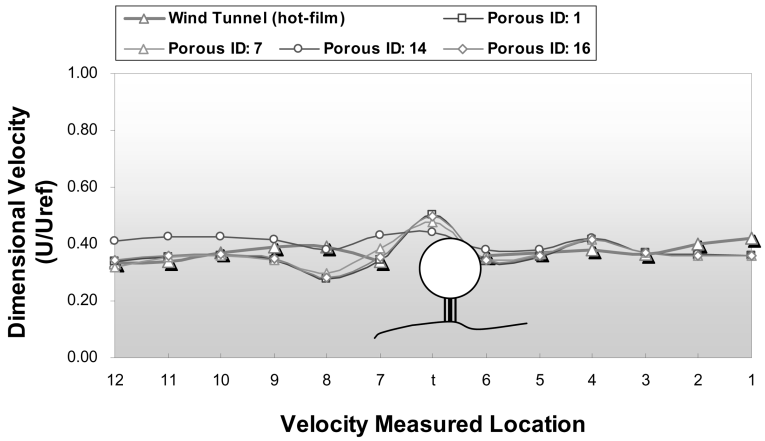

Fig. 6 Comparison of tree effects between wind tunnel test and CFD (Dimensionless wind velocity)

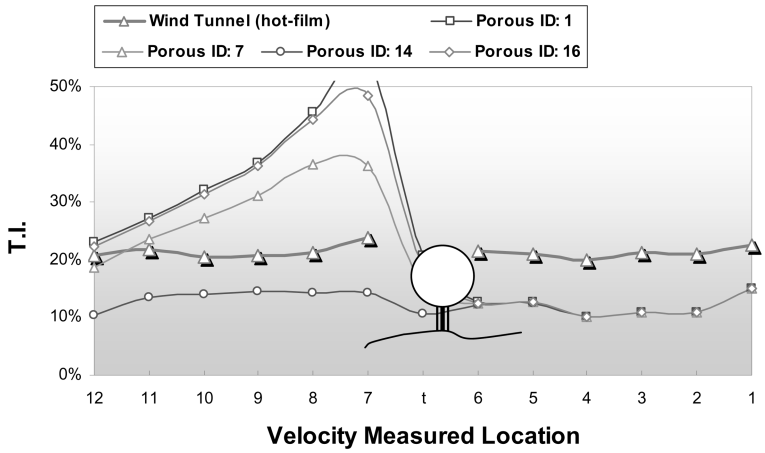

Fig. 7 Comparison of tree effects between wind tunnel test and CFD (Turbulence intensity)

and 7. The comparison results show that case of porous ID 7 had better fit comparing with wind tunnel data.

The final value of viscous resistance, C_2 and inertial resistance, $1/\alpha$ for pedestrian wind simulation were 4.557 and 130.21 respectively. These two values will used for CFD simulation of the completed model for case with tree consideration. Fig. 8 shows the photograph of the completed model in wind tunnel and configuration of main building, surrounding area, and trees of CFD model.

4. Results and conclusions

Many studies have shown that CFD well predicts wind tunnel results with optimum boundary condition, grid resolution and turbulence model. Moreover, this study shows that with trees adding to the calculation model, better predictions will result if the parameters of porous media condition

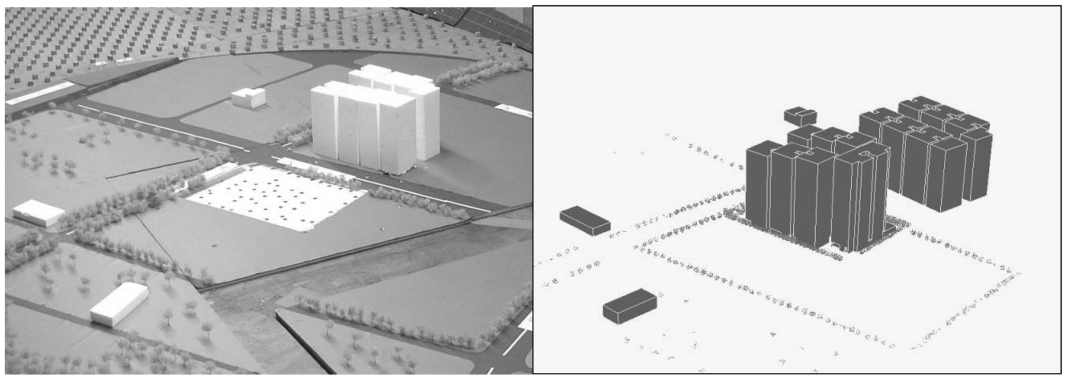

Fig. 8 Pedestrian wind tunnel test and CFD model

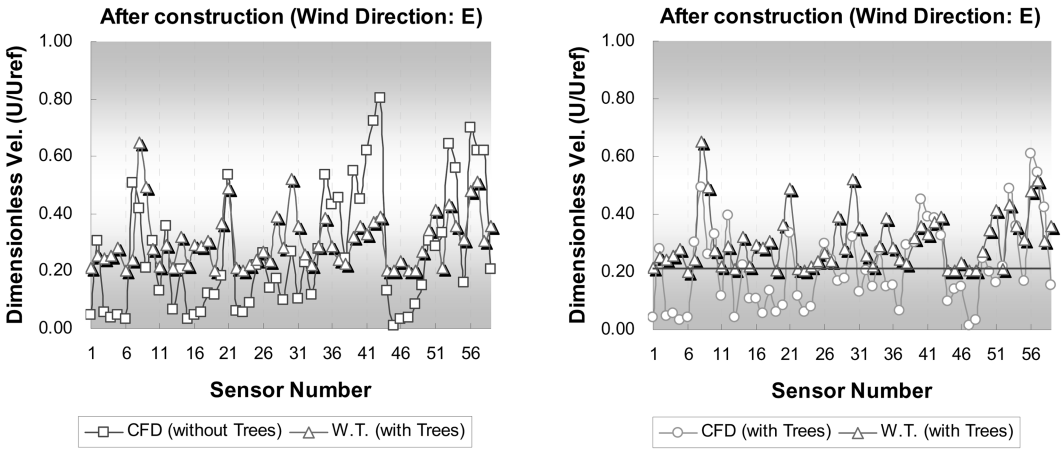

Fig. 9 Comparison between measured and calculated (w/o trees) dimensional velocity on pedestrian level

are well adjusted. In this study, only east approaching wind direction cases are investigated because east is the maximum wind velocity direction in Taiwan according to Taipei Meteorological Station. Fig. 9 shows a direct comparison between measured and calculated dimensional velocity on pedestrian level for all sensor location. The results indicate that the CFD predictions with trees including in the calculation better agree with wind tunnel data. The same analytical techniques are also used to examine two other cases. In Fig. 10, X-axis represents the wind tunnel results and Y-axis represents the CFD simulation results. It indicates that the results of CFD simulation with trees (triangle dots) fits better with the 45-degree line compare with the results of CFD simulation without trees. The correlation coefficient of CFD simulation with trees (triangle dots) and without trees (blue circle) were 0.65 and 0.56.

According to Fig. 9, most of the dimensionless velocities measured from Irwin sensors are higher than 0.2. However, CFD simulation also gives some predicting values of dimensionless velocities that are lower than 0.2. Irwin sensors have limitations on detecting low velocity winds due to low sensibilities, which affects the comparison accuracy of the wind tunnel models and CFD simulation models. For example, the differences between wind tunnel measurements and CFD predictions with

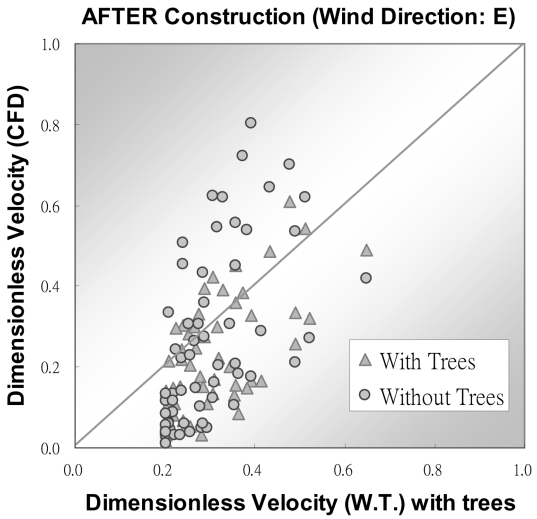

Fig. 10 Experimental vs. calculated (w/o trees)-dimensionless velocity

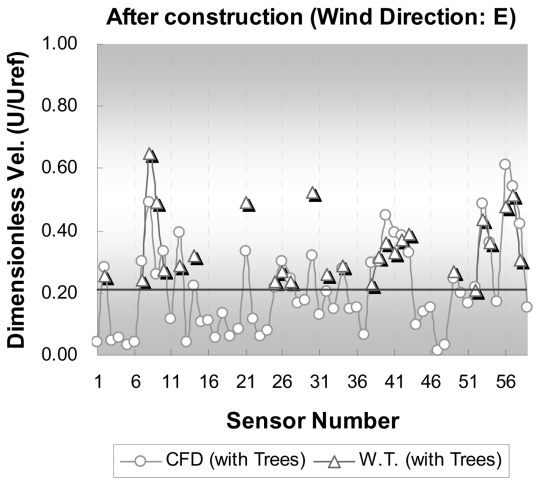

Fig. 11 Comparison between measured and calculated for dimensionless velocity > 0.2

trees in sensor numbers of 52, 56, and 58 are 0.329 (107%), 0.430 (144%), 0.448 (152%) respectively. Fig. 11 shows the comparison results after eliminating the dimensionless velocities that are lower than 0.2. Fig. 12 presents that the correlation of dimensionless velocity of wind tunnel with trees and dimensionless velocity of CFD with trees is better when *U*/*Uref* is greater than 0.2. The results indicate the better predictions after eliminating the data of *U*/*Uref* under 0.2. The correlation coefficient of CFD simulation with trees, all data and data of U/Uref >0.2 were 0.65 and 0.69. Fig. 13 shows the velocity contour, at pedestrian level, from CFD simulations with tree effects. Fig. 14 is the turbulence intensity contour from CFD simulations with tree effects. The results show the dimensionless velocity is reduced and T.I. is increased in the regions where trees are existed.

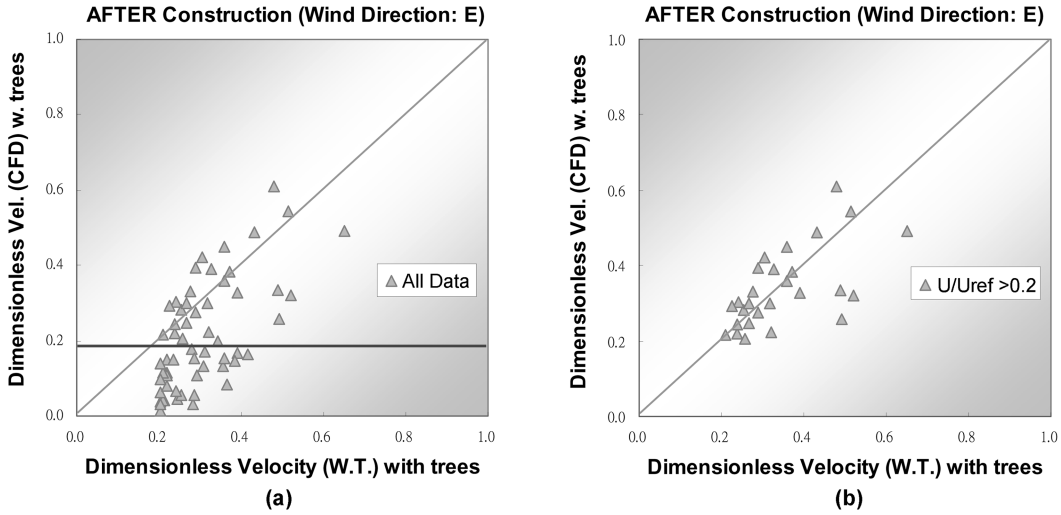

Fig. 12 Correlation between measured and CFD prediction with trees, (a) all data (b) *U*/*Uref* > 0.2

Fig. 13 Velocity contour, at pedestrian level, from CFD simulations with tree effects

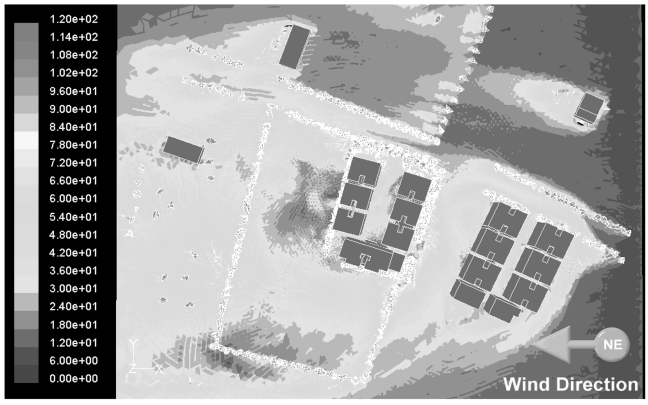

Fig. 14 Turbulence intensity contour, at pedestrian level, from CFD simulations with tree effects

Porous Media Condition is useful function to present the roadside trees in the numerical model without increasing the mesh grids. The numerical and wind tunnel models have reasonable match if the parameters of porous media condition are well adjusted.

References

Chang, C.H. and Meroney, R.N. (2001a), "Numerical and physical modeling of bluff body flow and dispersion in urban street canyons", *J. Wind Eng. Ind. Aerodyn*., **89** 1325-1334.

Chang, C.H. and Meroney, R.N. (2001b), "The effect of surroundings with different separation distances on surface pressures on low-rise buildings", *J. Wind Eng. Ind. Aerodyn*., **91** (2003), 1039-1050.

Ferreira, A., Sousa, A. and Viegas, D. (2002), "Prediction of building interference effects on pedestrian level comfort", *J. Wind Eng. Ind. Aerodyn*., **90**, 305-319.

Fluent 6: User's Guide, July 2002. Fluent Incorporated. Website: http://www.fluent.com.

He, J. and Song, C.C.S. (1999), "Evaluation of pedestrian winds in urban area by numerical approach", *J. Wind Eng. Ind. Aerodyn*., **81**, 295-309.

Hiraoka, H. (1993), "Modeling of turbulent flows within plant/urban canopies", *J. Wind Eng. Ind. Aerodyn*., **46 & 47**, 1759-1776.

Jamieson, N.J., Carpenter, P. and Cenek, P.D. (1992), "The effect of architectural detailing on pedestrian-level wind speeds", *J. Wind Eng. Ind. Aerodyn*., **41-44**, 2301-2312.

Mochida, A., Watanabe, H., Sakaida, K. Yoshino, H., Iwata, T. Hataya, N., Junimura, Y. and Shibata, K. (2004), "CFD analysis and field measurement of thermal environment and pollutant diffusion in street canyon-Investigation on the effects of roadside trees", *Proceedings of WERC International Symposium on Architectural Wind Engineering*, Nov. **18**, 135-147.

Murakami, S., Ooka, R., Mochida, A., Yoshida, S. and Kim, S. (1999), "CFD analysis of wind climate from human to urban scale", *J. Wind Eng. Ind. Aerodyn*., **81**, 57-81.

Murakami, S., Uehara, K. and Komine, H. (1979), "Amplification of wind speed at ground level due to construction of high-rise building in urban area", *J. Ind. Aerodyn*., **4**, 343-370.

Stathopoulos, T. and Baskaran, B. (1996), "Computer simulation of wind environmental conditions around buildings", *Eng. Struct.*, **18**(11), 876-885.

Stathopoulos, T. and Wu, H. (1995), "Generic models for pedestrian-level winds in built-up regions", *J. Wind Eng. Ind. Aerodyn*., **54/55**, 515-525.

Stathopoulos, T. and Wu, H. (2004), "Using computational fluid dynamics (CFD) for pedestrian winds", *Proceedings of the 2004 Structures Congress-Building on the past: Securing the Future*, 461-469.

Svensson, U. and Haggkvist, K. (1990), "A two-equation turbulence model for canopy flows", *J. Wind Eng. Ind. Aerodyn*., **35**, 201-211.

Uchida, T. and Ohya, Y. (1999), "Numerical simulation of atmospheric flow over complex terrain", *J. Wind Eng. Ind. Aerodyn*., **81**, 283-293.

CC